Biophysical Chemistry 247 (2019) 13–24

Contents lists available at ScienceDirect

Biophysical Chemistry

journal homepage: www.elsevier.com/locate/biophyschem

Cooperative energetic effects elicited by the yeast Shwachman-Diamond syndrome protein (Sdo1) and guanine nucleotides modulate the complex conformational landscape of the elongation factor-like 1 (Efl1) GTPase

Axel Luviano, Roberto Cruz-Castañeda, Nuria Sánchez-Puig*, Enrique García-Hernández*

Universidad Nacional Autónoma de México, Instituto de Química, Ciudad Universitaria, Ciudad de México 04510, Mexico

HIGHLIGHTS

- Recognition energetics of Efl1 in solution was determined by ITC.
- Sdo1 increases 70-fold the relative affinity of Efl1 for GTP over that for GDP.
- Depending on the ligand(s), Efl1 shows at least 4 evidently different conformations.
- Efl1 conformation bound to GTP and/or Sdo1 is more compact than that bound to GDP.
- Conformational landscape of Efl1 is modulated similarly to translational GTPases.

GRAPHICAL ABSTRACT

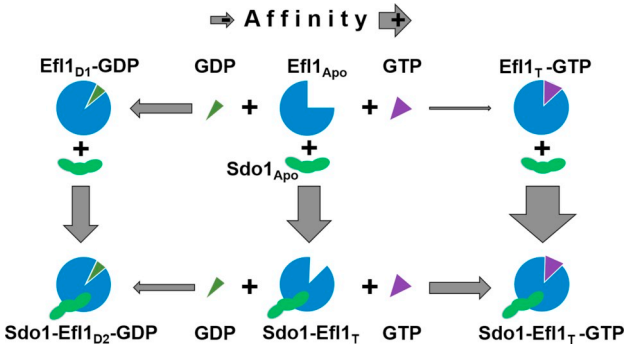

ARTICLE INFO

Keywords:
Efl1/EFL1
Sdo1/SBDS
Guanine nucleotide
Isothermal titration calorimetry
Conformational change
Binding heat capacity

ABSTRACT

One of the final maturation steps of the large ribosomal subunit requires the joint action of the elongation factor-like 1 (human EFL1, yeast Efl1) GTPase and the Shwachman-Diamond syndrome protein (human SBDS, yeast Sdo1) to release the eukaryotic translation initiation factor 6 (human eIF6, yeast Tif6) and allow the assembly of mature ribosomes. EFL1 function is driven by conformational changes. However, the nature of such conformational changes or the mechanism by which they are prompted are still largely unknown. In previous studies, it has been established that this GTPase interacts with its cofactor in solution in an inverted orientation with respect to the binding mode derived from 60S ribosome subunit cryo-EM data. To shed new light on this conundrum, we characterized calorimetrically the energetic basis describing the recognition of Efl1 to GT(D)P, Sdo1 and their intercommunication in solution. A structural-based analysis of the binding signatures indicates that Efl1 has a large structural flexibility. The mutual effects of Sdo1 and nucleotides on Efl1 modulate in a very specific and robust way the complex conformational landscape of Efl1, resembling the behavior observed with other GTPases and their cofactors.

Abbreviations: EFL1, human elongation factor like-1 protein; Efl1, yeast elongation factor like-1 protein; SBDS, human Shwachman-Diamond syndrome protein; Sdo1, yeast Shwachman-Diamond syndrome protein; eIF6, eukaryotic initiation factor 6; SDS, Shwachman-Diamond syndrome; ITC, isothermal titration calorimetry; GDP, guanosine diphosphate; GTP, guanosine triphosphate; GMPPNP, 5′-guanylyl imidodiphosphate

* Corresponding authors.
E-mail addresses: nuriasp@unam.mx (N. Sánchez-Puig), egarciah@unam.mx (E. García-Hernández).

https://doi.org/10.1016/j.bpc.2019.02.003
Received 1 January 2019; Received in revised form 31 January 2019; Accepted 6 February 2019
Available online 13 February 2019

1. Introduction

Ribosome synthesis is an intricate multistep process through which the assembly of ribosomal subunits is orchestrated by numerous accessory proteins [1–3]. In eukaryotic cells, one of the last maturation steps of the 60S subunit prior to its incorporation into fully functional ribosomes requires the release of the translation initiation factor 6 (human eIF6, yeast Tif6) [4]. This event is coordinated by the cooperative action of the elongation factor-like 1 (human EFL1, yeast Efl1) GTPase and its cofactor the Shwachman-Diamond syndrome protein (human SBDS, yeast Sdo1) [5–7]. SBDS promotes an allosteric conformational change in EFL1 that causes the steric displacement of eIF6 from the surface of the 60S subunit. Mutations that impair correct communication between SBDS and EFL1 prevent the release of eIF6, obstructing the assembly of actively translating ribosomes and leading to the progression of the human ribosomopathy known as Shwachman-Diamond syndrome (SDS) [8–10].

EFL1 is a large GTPase (1110 residues for the yeast orthologue) phylogenetically related to the prokaryotic ribosomal translocase EF-G and the eukaryotic elongation factor EF-2 [11]. These GTPases are organized in five structurally dissimilar domains, although the EFL1 protein family has an insertion of variable length in domain II (79 and 160 residues in the human and yeast orthologues, respectively) that is absent in EF-G or EF-2. SBDS is a relative small assembly factor (250 residues) with a highly flexible three-domain architecture [5,12,13]. A recent cryo-electron microscopy study of 60S ribosomal subunit structures complexed with SBDS-eIF6, SBDS-EFL1-eIF6 or SBDS-EFL1 has provided significant insights into the mechanism of eIF6 release through the concerted action of SBDS and EFL1 [14]. In this study, the authors propose that the last stage of ribosome maturation initiates when the eIF6-bound pre-60S subunit becomes able to interact with SBDS after recruitment of the last structural ribosomal protein uL16 and release of the nuclear export factor Nmd3 by the GTPase Lsg1. eIF6 occupies a site on the ribosome surface composed of the sarcin-ricin loop (SRL) and segments of the uL14, uL3 and eL24 proteins. SBDS binds in a region comprised by the tRNA P-site and the base of the stalk, making no contact with the anti-association factor. The region between SBDS and eIF6 corresponds to the ribosome GTPase center, which is subsequently occupied by EFL1 in a low-affinity GTP-bound state. In the SBDS-EFL1-eIF6 complex, domains III and IV of EFL1 directly interact with domains II and III of SBDS, while domains I and II of the GTPase, far away from the SBDS-EFL1 interface, contact eIF6. Upon undergoing an SBDS-dependent conformational change, EFL1 adopts a competent state in which domain I (the GTPase domain), along with the characteristic insertion loop in domain II, sterically displaces eIF6 from the ribosome. It is thought that GTP hydrolysis elicits a conformational shift that finally triggers the liberation of the GTPase and its cofactor. This mechanism not only prevents premature association of the ribosomal subunits, but also provides a final quality control point to assess the integrity of key functional 60S subunit sites, namely, the polypeptide exit tunnel, the P site, the GTPase center, the base of the P-stalk and SRL.

The above model for the last maturation step of the 60S subunit represents a milestone in understanding the molecular basis of ribosomal biogenesis, as well as in the elucidation of key determinants for the progression of SDS. Nevertheless, several aspects of the process have yet to be elucidated. For instance, other structural and genetic studies using the yeast orthologues suggest that the release of Nmd3 and Tif6 is coupled rather than sequential [15–17]. In this other model, the interaction between Tif6 and Nmd3 needs to be disrupted most probably by Efl1 for the latter to retract from the L1 stalk (uL1) and promote the release of both accessory factors in a concerted manner. Clarifying or maybe unifying these models will require further investigation. The precise timing for the recruitment of EFL1 to the ribosome has not been clarified, nor the influence of the nucleotides and/or SBDS in this process. Furthermore, the energetics that govern the cascade of conformational events that end in the release of eIF6 has not been determined, which prevents a quantitative description of the underlying molecular forces. In addition, there is still scarce information about the cooperative effects between nucleotides and SBDS in regulating the conformational landscape of EFL1, and the mechanism that drives the eviction of these proteins from the 60S subunit.

The mechanism derived from the cryo-EM structures postulates a binding mode between SBDS and EFL1 in which the GTPase adopts an opposite orientation to that inferred from earlier studies carried out in a ribosome-free context. Calorimetric measurements of the association between Sdo1 and Efl1 and truncated constructs of these yeast orthologues prove that the insertion loop in domain II of the GTPase interacts directly with domains II-III of the cofactor [18]. An Efl1 construction deleted of its insertion loop is unable to interact with Sdo1, while the isolated loop binds to the cofactor with great affinity [18]. Further studies have established that for binding to Sdo1, it is not only this insertion in Efl1 that is important but domains I and II are also important [19]. Additionally, some SBDS missense mutations implicated in SDS that modify surface epitopes without perturbing the protein fold weaken the interaction with EFL1 in vitro [19]. These results correlate with mass spectrometry experiments showing a direct contact between residues Met^{435} in the Efl1 insertion loop and Ser^{143} in the Sdo1 domain II [20]. Ser^{143} is a residue whose Leu or Trp variants are associated with SDS and result in the loss of affinity between SBDS and EFL1 in solution [21]. In contrast, the models derived from cryo-EM data pose SBDS Ser^{143} 60 Å away from EFL1 Ala^{439} (Efl1 Met^{435}). Overall, the binding mode of Sdo1 and Efl1 determined from solution studies is drastically different from that proposed by cryo-EM data regarding the orientation of the GTPase. In the former, the insertion loop forms part of the protein-protein interface, while in the latter the insertion loop lies far away from that interface occupying a position where it seems to play a direct role in the displacement of eIF6. In vivo, however, yeast cells complemented with Efl1 lacking this insertion show no apparent growth defect questioning the role of this region on the release of Tif6 [14]. Furthermore, the insertion is not a conserved feature within the EFL1 protein family; for instance, it is almost inexistent in the proteins of the protists *Toxoplasma gondii* and *Plasmodium sp.*, but is amongst the longest in the human and yeast orthologues.

A binding kinetic study with the yeast orthologues Sdo1 and Efl1 using fluorescent analogues of guanine nucleotides showed that Sdo1 weakens the interaction of Efl1 with GDP [21]. Therefore, it was proposed that Sdo1 acts as a guanine exchange factor (GEF) for Efl1. In this study, it was also shown that Efl1 undergoes structural rearrangements upon nucleotide binding. However, the extent and nature of these changes were not described, nor their reliance on Sdo1 and/or the nucleotide type. To further clarify the communication between Sdo1 and Efl1 off the ribosome, and the impact of this interaction on the recognition of guanine nucleotides, in this work we characterized the molecular recognition thermodynamics of Efl1 by isothermal titration calorimetry. This technique allowed a straightforward determination of the complete thermodynamic binding signatures, without the need for extrinsic reporters that might alter the interaction. In addition, by performing the measurements at different temperatures it was possible to quantify the binding heat capacity (ΔCp_b) of the different complexes with precision. This thermodynamic function relates to the reorganization of the solvent around protein and ligand surfaces, and it is therefore an excellent reporter on the extent of the conformational changes occurring upon complex formation [22–25]. Our data revealed a complex conformational landscape of the GTPase which is finely regulated by Sdo1 and both guanine nucleotides, GTP and GDP. Importantly, the mutual effects of Sdo1 and nucleotides on Efl1 parallel the behavior observed for other GTPases and their cofactors. In view of these results, further investigation about the possible functional role of these interactions off the ribosome is clearly warranted.

$$
\begin{array}{ccccccccc}
 & & & K_{M\text{-}G},\Delta H_{M\text{-}G} & & & & K_{MG\text{-}M},\Delta H_{MG\text{-}M} & \\
GT(D)P & + & 2Mg(II) & \leftrightarrow & Mg-GT(D)P & + & Mg(II) & \leftrightarrow & Mg_2-GTP \\
+ & & & & + & & & & \\
E & K_{E\text{-}G},\Delta H_{E\text{-}G} & & & E & K_{E\text{-}MG},\Delta H_{E\text{-}MG} & & & \\
\updownarrow & & & & \updownarrow & & & & \\
E-GT(D)P & + & 2Mg(II) & \leftrightarrow & E-MgGT(D)P & + & Mg(II) & & \\
 & & & K_{EG\text{-}M},\Delta H_{EG\text{-}M} & & & & &
\end{array}
$$

Scheme 1. Ternary binding equilibrium between Efl1 (E), Mg(II) ions and GT(D)P. The ability of GTP to bind to two Mg(II) ions is explicitly taken into account.

2. Materials and methods

2.1. Protein samples

Yeast Efl1 and Sdo1 proteins were recombinantly produced and purified as described elsewhere [26]. In brief, the Efl1 protein sequence (NP_014236) was fused to a TEV protease cleavage site at the C-teminus followed by a 6xHis-tag and cloned into pRS426 vector [27] under the control of the *GAL1/10* promoter. Recombinant protein expression was induced in *S. cerevisiae* BCY123 with galactose and purified by affinity chromatography using His-Trap-FF column (GE Healthcare), treated with TEV protease (0.05 mg/g of fusion protein), followed by a second affinity chromatography and a final size exclusion chromatography using a HiLoad 16/600 Superdex 200 column (GE Healthcare). Final yield corresponded to 5 mg of protein/l of culture of pure recombinant Efl1 protein as determined by SDS-PAGE and MALDI-TOF spectrometry. The yeast Sdo1 coding sequence (NP_013122) was cloned into pRSET-A vector (Invitrogen) fused to a 6xHis-tag at the N-terminus. Purification of the recombinant Sdo1 protein was done by affinity chromatography followed by ion exchange chromatography with HiTrap-SP-Sepharose FF column (GE Healthcare) to yield 10 mg of protein/l of culture. All experiments were performed with freshly purified protein.

2.2. Circular dichroism spectroscopy (CD)

The CD spectra of Efl1 and Sdo1 were recorded at 20 °C in the far-UV region with a JASCO J-720 spectropolarimeter (Jasco Inc., Easton, MD) equipped with a PTC-348WI Peltier-type cell holder for temperature control. Protein solutions of ~0.2 mg/ml were loaded into a quartz cell of 0.1-cm length path. Each spectrum corresponds to the average of three repetitive scans and was corrected by the buffer signal. Ellipticities are reported as mean residue ellipticity, $[\theta]_{mrw}$. Secondary structure content was calculated from CD spectra using the deconvolution software K2D3 [28]. Thermal denaturation transitions were followed by monitoring the ellipticity signal at 208 nm, using a constant scan rate of 1 °C/min. Unfolded fractions as a function of temperature ($f_U(T)$) were calculated as:

$$f_U(T) = \frac{\theta(T) - \theta_N(T)}{\theta_U(T) - \theta_N(T)} \quad (1)$$

where $\theta(T)$, $\theta_N(T)$ and $\theta_U(T)$ are the observed, native and unfolded ellipticities, respectively.

2.3. Isothermal titration calorimetry (ITC)

Calorimetric measurements for the titration of Efl1 with guanine nucleotides or Sdo1 were carried out using a MicroCal™ iTC_{200} System (GE Healthcare, Northampton, MA, USA). Unless otherwise stated, all the experiments were performed in a 0.05 M Tris-HCl buffer solution, pH 8.0, supplemented with 0.1 M NaCl, 125 μM DTT, and 10% glycerol. At each temperature measurement, the pH was adjusted to maintain it at a constant value of 8.0. Efl1 concentration in the cell comprised 25–30 μM, while ligand concentrations in the syringe were: 2 mM for GTP or MgGTP, 1.0–1.5 mM for GDP or MgGDP, and 0.5–1.0 mM for Sdo1. For the titration of Efl1 with Mg(II)-bound GT(D)P, both the ligand and protein solutions contained 5 mM $MgCl_2$. In the case of the titrations with Mg(II)-free nucleotide, ligand and protein solutions were supplemented with 2 mM EDTA to sequester any residual trace of the metal ion in the solution. The titration schedule consisted of 15–20 consecutive injections of ligand with a 5-min interval between injections, using a stirring rate of 750 rpm. The dilution heat of the ligand was obtained by adding ligand to a buffer solution under identical conditions and the same injection schedule used to that with the protein sample. All samples were degassed for 10 min prior to the experiment.

The resulting binding isotherms for the isolated GTPase obtained in presence of Mg(II) were analyzed using a ternary model in which free Efl1 (E) may bind GT(D)P or MgG(D)TP, while GTP may also be in the form of Mg_2GTP (Scheme 1)

Subscripts M-G and MG-M stand for the stepwise association of two magnesium ions to the guanine nucleotide, *E*-G and E-MG for the association of metal-free and metal-bound guanine nucleotide to the enzyme, and EG-M for the association of Mg(II) to the nucleotide-prebound protein, respectively. In this coupled equilibrium of weak interactions, GT(D)P and MgGT(D)P compete with each other for the Efl1 binding site. Derivation of the coupled-equilibria model has been presented in detail elsewhere [29]. In brief, the heat involved at each step of the titration is described by:

$$
\begin{aligned}
q_i = V_0\Bigg(&\left([E\bullet GT(D)P]_i - [E\bullet GT(D)P]_{i-1}\left(1 - \frac{v_i}{V_0}\right)\right)\Delta H_{E-G} \\
&+ \left([E\bullet MgGT(D)P]_i - [E\bullet MgGT(D)P]_{i-1}\left(1 - \frac{v_i}{V_0}\right)\right)(\Delta H_{E-MG} \\
&+ \Delta H_{M-G}) + \Bigg([MgGT(D)P]_i - [MgGT(D)P]_{i-1}\left(1 - \frac{v_i}{V_0}\right) \\
&- F_{MgGT(D)P}[GT(D)P]_0\frac{v_i}{V_0}\Bigg)(\Delta H_{M-G}) \\
&+ \Bigg([Mg_2GTP]_i - [Mg_2GTP]_{i-1}\left(1 - \frac{v_i}{V_0}\right) \\
&- F_{Mg_2GTP}[GTP]_0\frac{v_i}{V_0}\Bigg)(\Delta H_{M-G} + \Delta H_{MG-M})\Bigg) + q_{dil}
\end{aligned} \quad (2)
$$

where q_i stands for the heat evolved in the *i*-th injection, V_o is the working volume of cell, v_i is the aliquot volume added at injection *i*, and q_{dil} is a fitting term introduced to account for experimentally uncorrected dilution heat effects. For GDP, the binding parameters for the second metal ion were set to zero. $F_{MgGT(D)P}$ and F_{Mg2GTP} correspond, respectively, to the fraction of MgGT(D)P and Mg_2GTP complexes in the syringe introduced in the cell just by injection. Finally, $[GT(D)P]_0$ stands for the GT(D)P concentration in the syringe.

The total concentration of each species in Eq. 2 is related to the concentration of the free molecular counterparts through the corresponding equilibrium constant:

$$
\begin{aligned}
[GT(D)P]_T &= [GT(D)P] + K_{M-G}[GT(D)P][Mg(II)] \\
&\quad + K_{M-G}K_{MG-M}[GT(D)P][Mg(II)]^2 \\
&\quad + K_{E-G}[E][GT(D)P] + K_{E-MG}K_{M-G}[E][GT(D)P][Mg(II)] \\
[Mg(II)]_T &= [Mg(II)] + K_{M-G}[GT(D)P][Mg(II)] \\
&\quad + 2K_{M-G}K_{MG-M}[GTP][Mg(II)]^2 \\
&\quad + K_{E-G}K_{M-G}[E][GT(D)P][Mg(II)] \\
[E]_T &= [E] + K_{E-G}[E][GT(D)P] + K_{E-MG}K_{M-G}[E][GT(D)P][Mg(II)]
\end{aligned}
\tag{3}
$$

During fitting to this ternary model, formation parameter values $K_{E\text{-}G}$, $\Delta H_{E\text{-}G}$ for the complexes of GT(D)P with free Efl1, $K_{M\text{-}G}$, $\Delta H_{M\text{-}G}$ for MgGT(D)P and $K_{MG\text{-}M}$, $\Delta H_{MG\text{-}M}$ for Mg_2GTP were kept fixed (determined in independent experiments), while $K_{EG\text{-}M}$, $\Delta H_{EG\text{-}M}$ for the interaction with MgGT(D)P were the fitting parameters. We assumed that the interaction parameters of Mg(II) with guanine nucleotides are similar to those with adenine nucleotides and therefore we used the previously reported values for the latter [29]. Binding parameters for the interaction of metal-free nucleotides with Efl1 were determined using an identical and independent binding site model [30,31] according:

$$
Q = \frac{M_t \Delta H_{E-G} V_O}{2}\left[1 + \frac{L_t}{M_t} + \frac{1}{K_{E-G}M_t} - \sqrt{\left(1 + \frac{L_t}{M_t} + \frac{1}{K_{E-G}M_t}\right)^2 - \frac{4L_t}{M_t}}\right] \tag{4}
$$

where Q is the normalized heat evolved per mol of ligand at the end of the i^{th} injection, and L_t and M_t are the total ligand and macromolecule concentration, respectively. The heat released in the i^{th} injection is:

$$
q_i = Q_i + \frac{v_i(Q_i + Q_{i-1})}{2V_O} - Q_{i-1} + q_{dil} \tag{5}
$$

For the titration of Sdo1-bound Efl1 with Mg(II)-free GT(D)P, the underlying coupled equilibria model is described by Scheme 2, in which free and Sdo1-bound Efl1 (E and *E*-P, respectively) may bind the nucleotide:

Binding parameters for the interaction of Sdo1 with Efl1 ($K_{E\text{-}S}$, $\Delta H_{E\text{-}S}$) were determined from direct binary titration experiments, by non-linear fitting of Eqs. 4 and 5 to the normalized titration data. For the ternary interaction of Efl1, Sdo1 and nucleotide, the binding model adopted a similar form to that described by Eqs. 3 and 4. To bias the experimental setup for predominantly measuring the interaction of the complex Efl1-Sdo1 (*E*-S) with the nucleotide, a three-fold concentration excess of Sdo1 was used compared to that of Efl1. Considering the dissociation constant measured in this work, this results in > 99% of Efl1 bound to Sdo1 prior to addition of the nucleotide.

Finally, fitting to the experimental data included a parameter n as normalization factor to correct for errors in the quantification of protein concentration and/or to account for the presence of inactive protein fraction:

$$
[E]_T = n[E]_0 \tag{6}
$$

where $[E]_0$ is the experimental concentration of Efl1.

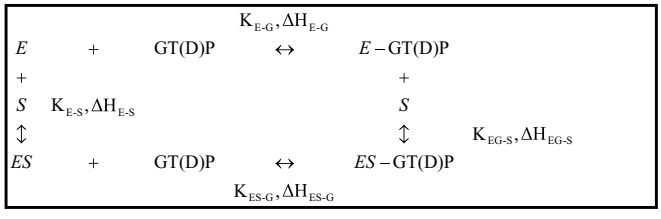

Scheme 2. Ternary binding equilibrium between Efl1 (E), Sdo1 (S) and GT(D)P.

All non-linear regressions were carried using the program Origin 7.0 (OriginLab, Co., Northampton, MA) and the Affinimeter software (www.affinimeter.com) [32].

The heterotropic cooperativity in the binding of nucleotide and Mg(II) to Efl1 is contained in $K_{E\text{-}MG}$ and $\Delta H_{E\text{-}MG}$ relative to $K_{E\text{-}G}$ and $\Delta H_{E\text{-}G}$ values [29]:

$$
\kappa = K_{E-MG}/K_{E-G} = K_{EG-M}/K_{M-G} \tag{7}
$$

$$
\Delta h = \Delta H_{E-MG} - \Delta H_{E-G} = \Delta H_{EG-M} - \Delta H_{M-G} \tag{8}
$$

Finally, the cooperative entropy change can be calculated as:

$$
T\Delta s = \Delta h - \Delta g = \Delta h + RT\ln\kappa \tag{9}
$$

Corresponding expressions apply to the heterotropic cooperativity for the binding of nucleotides and Sdo1 to Efl1.

2.4. Changes in accessible surface area

The protein data bank (PDB) was surveyed for experimentally solved structures of translation GTPases in complex with guanine nucleotides. Three GTPases bound to GDP were found (EF-G PDB:1DAR [33], eEFSec PDB:5IZK [34], Hbs1 PDB:3P27 [35]), four bound to MgGDP (EF-G PDB:1FNM [36], EF-Tu PDB:1TUI [37], eIF5B PDB:4NCF and 4NCL [38]), two bound to GTP/GMPPNP (eIF5B PDB:4NCN [38] and eEF2 PDB:2E1R [39]) and two bound to MgGMPPNP (EF-Tu PDB:1EFT [40] and 1EXM [41]), and EF-Pyl PDB:3WNB [42]). Structure-based determinations of water-accessible surface areas (ASA) were performed with the NACCESS program [43], using a probe radius of 1.4 Å and a slice width of 0.25 Å. Assuming a rigid-body like association, changes in accessible surface area (ΔASA) upon formation of each GTPase-nucleotide complex were estimated considering the difference between the complex and the sum of the free molecular partners. Polar (ΔASA_p) and apolar (ΔASA_{ap}) area changes were calculated from changes in accessibility of nitrogen plus oxygen atoms and sulfur plus carbon atoms, respectively. Magnesium and phosphate areas were considered as polar areas.

3. Results

3.1. Thermal stability of Efl1 and Sdo1

To establish the appropriate experimental temperature interval to perform the ITC measurements, the thermal unfolding profiles of Efl1 and Sdo1 were determined by CD spectroscopy. The far-UV CD spectra of both proteins recorded at room temperature consisted of the typical signals of folded proteins (Fig. 1). Deconvolution of the CD spectra indicated fractional contents of α-helix/β-strand conformations of 0.28/0.14 and 0.36/0.09 for Efl1 and Sdo1, respectively. These secondary structure contents are in good agreement with those observed in the cryo-EM structures of the human EFL1 (0.30/0.09) and SBDS (0.39/0.15) bound to the ribosomal 60S-subunit [14], and in the NMR structures of the isolated human SBDS [5]. The inset in Fig. 1 shows the thermal denaturation profiles. Both proteins exhibited a sharp transition, providing additional evidence that, as isolated entities, they are natively-like folded. Sdo1 was more resistant to thermal perturbation than Efl1, with an unfolding onset of ~60 °C, while that of the GTPase was ~40 °C. Since the pH of a Tris buffer solution has a significant dependence on temperature, a melting curve for Efl1 in a phosphate buffer was also recorded. In this last buffer, the unfolding onset was also ~40 °C, while the midpoint transition occurred ~4 °C below that observed in the Tris buffer. Therefore, we decided to set 30 °C as the upper temperature limit to carry out the titration measurements.

3.2. Binding energetics of Efl1 to guanine nucleotides

As shown in Scheme 1 for the binding of Efl1 to GT(D)P, several equilibria occur during the interaction of a protein with Mg(II)-bound

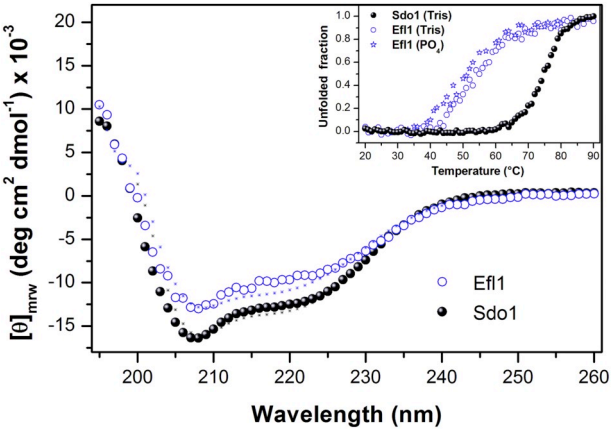

Fig. 1. Far-UV CD spectra of Efl1 (open symbols) and Sdo1 (solid symbols) at 20 °C. Asterisks represent the best-fitted spectra calculated using the deconvolution software K2D3. Inset: Thermal perturbation profiles determined from the change in ellipticity at 208 nm carried out in 15 mM Tris (circles) or 15 mM phosphate (stars) buffer, pH 8.

nucleotides. The simultaneous consideration of all coupled equilibria is required to obtain the actual thermodynamic values [29,44–46]. Fig. 2 shows representative examples of the calorimetric isotherms obtained for the Efl1-nucleotide complexes characterized in this work. For the interaction with metal-free GT(D)P in which a 1:1 equilibrium is established, a single binding site model was used to fit to the titration curves. In the presence of Mg(II), a model that considers the formation of all the species depicted in Scheme 1 was fitted to the data. Table 1 summarizes the values of the binding parameters as a function of temperature. Measurements carried out using buffers of different ionization enthalpy (ΔH_{ion} [47]) yielded the same binding enthalpy (within the experimental uncertainty), indicating that there is no binding-linked protonation event (Fig. 3).

The binding parameters for both nucleotides to isolated Efl1 exhibited a significant dependence on temperature. At 30 °C, the MgGDP affinity was three times larger than that for MgGTP. Although five times smaller, this affinity difference is consistent with that reported by García-Márquez et al. [21] for fluorescent mant-nucleotide derivatives at 28 °C. The affinity variation between the two nucleotides was due to small differences in the enthalpic and entropic contributions. Compared to the diphosphate, the triphosphate showed a larger favorable binding enthalpy (~1 kcal mol^{-1}) that was outweighed by a less favorable

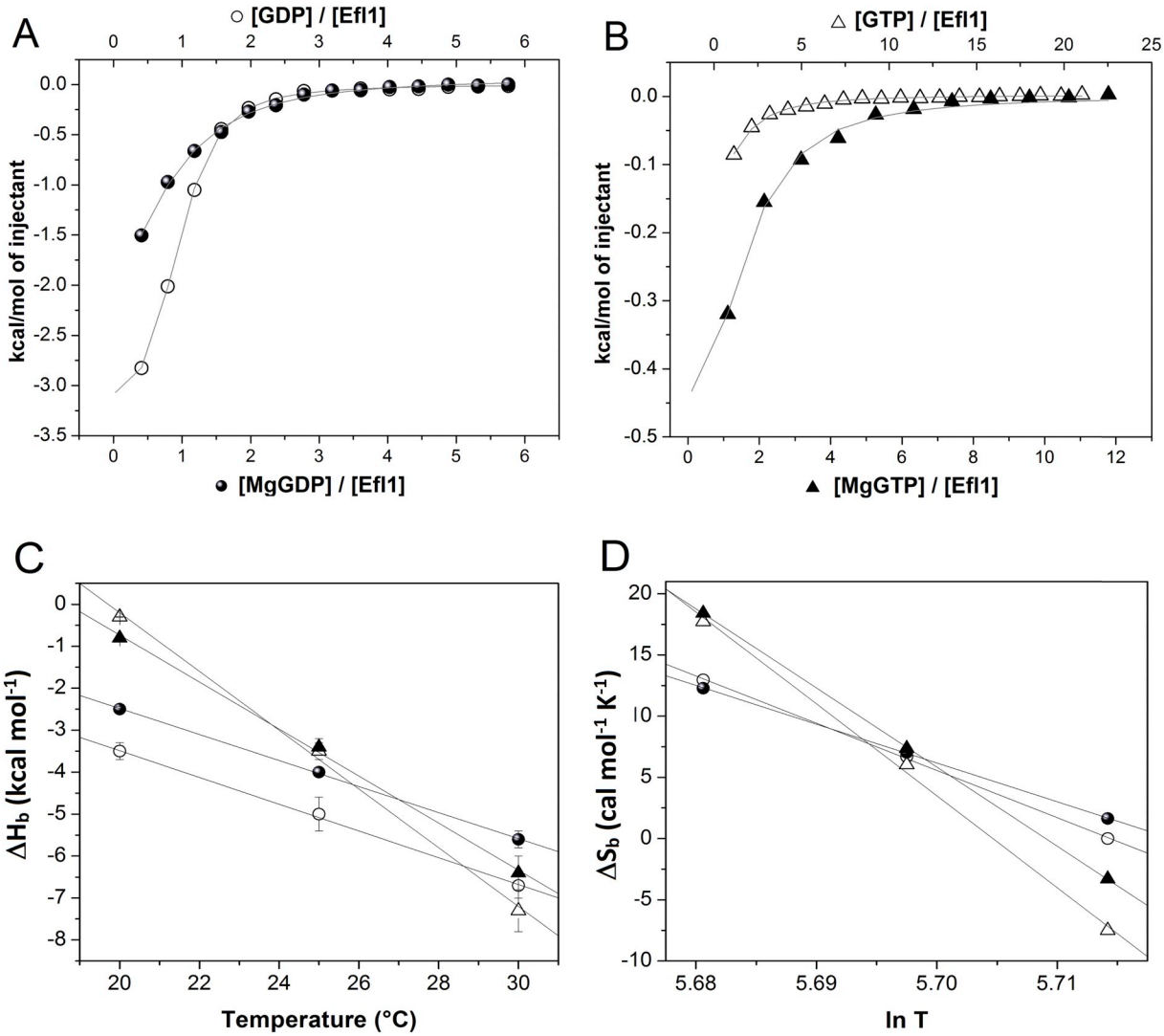

Fig. 2. Calorimetric characterization of the binding of Efl1 to GDP (○), MgGDP (●), GTP (Δ) and MgGTP (▲). Binding isotherms with (A) GDP/MgGDP and (B) GTP/MgGTP at 20 °C. Binding enthalpy (C) and entropy (D) as a function of temperature. Dashed lines correspond to the least squares linear fittings for describing the thermal dependence of ΔH_b or ΔS_b, i.e., assuming that ΔCp_b is constant in the temperature range spanned.

Table 1
Thermodynamic parameters for the binding of Efl1 to guanine nucleotides determined by ITC.

Ligand	T (°C)	n	K_b (mM^{-1})	K_d (μM)	ΔG_b (kcal mol^{-1})	ΔH_b (kcal mol^{-1})	$-T\Delta S_b$ (kcal mol^{-1})	ΔCp_b (cal mol^{-1} K^{-1})
GDP	20	0.90 ± 0.05	272 ± 11	4 ± 0.2	−7.3	−3.5 ± 0.2	−3.8	
	25	0.94 ± 0.02	141 ± 12	7 ± 0.5	−7.0	−5.0 ± 0.4	−2.0	−318 ± 35
	30	0.91 ± 0.02	64 ± 9	16 ± 2.2	−6.7	−6.7 ± 0.3	0.0	
MgGDP	20	0.95 ± 0.05	34 ± 2	29 ± 1.7	−6.1	−2.5 ± 0.1	−3.6	
	25	0.91 ± 0.02	32 ± 3	31 ± 2.9	−6.1	−4.0 ± 0.1	−2.1	−310 ± 5
	30	0.92 ± 0.02	27 ± 3	37 ± 4.1	−6.1	−5.6 ± 0.2	−0.5	
GTP	20	1.10 ± 0.08	12 ± 0.9	83 ± 6.2	−5.5	−0.3 ± 0.0	−5.2	
	25	1.01 ± 0.05	8 ± 0.7	125 ± 11	−5.3	−3.5 ± 0.3	−1.8	−700 ± 34
	30	1.02 ± 0.05	4 ± 0.3	250 ± 19	−5.0	−7.3 ± 0.3	2.3	
MgGTP	20	1.20 ± 0.08	45 ± 5	22 ± 2.4	−6.2	−0.8 ± 0.0	−5.4	
	25	1.11 ± 0.02	15 ± 2	66 ± 8.8	−5.7	−3.4 ± 0.0	−2.3	−560 ± 23
	30	1.09 ± 0.02	8 ± 0.7	125 ± 11	−5.4	−6.4 ± 0.4	1.0	

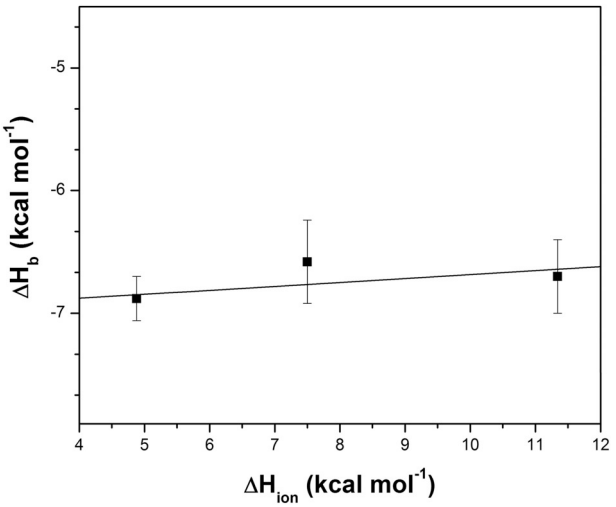

Fig. 3. Binding enthalpy as a function of the ionization enthalpy of the buffer. Independent titrations of Efl1 with GDP were performed using 0.05 M HEPES (ΔH_{ion} = 4.88 kcal mol^{-1}), 0.05 M Tricine (ΔH_{ion} = 7.5 kcal mol^{-1}) or 0.05 M Tris (ΔH_{ion} = 11.34 kcal mol^{-1}), pH 8.0, 30 °C. A linear regression analysis (solid line) yielded a net exchange of 0.03 ± 0.05 protons.

binding entropy (~1.5 kcal mol^{-1}). The greater thermal dependence shown by MgGTP resulted on the binding being both enthalpically and entropically driven at 20 °C to be only enthalpically driven at 30 °C. Interaction with MgGDP had a smaller dependence on temperature, and as a consequence, the binding strengths of the two nucleotides varied distinctively with temperature, with that of MgGTP being somewhat stronger at 20 °C.

The mutual effect of nucleotides and Mg(II) on the binding to Efl1 is contained in the magnitude of the cooperative heterotropic association constant (κ), which is defined by the ratio of the metal-bound to the metal-free nucleotide binding constants (Eqs. 7–9, Table 2). Magnesium ion increased the affinity of Efl1 for GTP although this effect was weakened as the temperature increased (κ(20 °C) = 3.8, κ(30 °C) = 2). Likewise, a positive heterotropic effect between Mg^{2+} and GTP has been observed for the translational GTPase eRF3 bound to its GEF protein eRF1 (κ(25 °C) = 5.5) [48]. On the contrary, the presence of the metal ion destabilized the interaction with GDP as shown for κ values smaller than 1, which increased with temperature (κ(20 °C) = 0.1, κ(30 °C) = 0.4). This behavior parallels the thermal trend observed previously for the translational GTPase eIF5B (κ(5 °C) = 0.3, κ(25 °C) = 0.5) [38] and the single temperature determination for eRF3 (κ(25 °C) = 0.6) [48]. Thus, all these data indicate that the γ-phosphate moiety is required to fulfill Mg(II) coordination at the active site of Efl1 and other translational GTPases. Nevertheless, it is noteworthy that the stronger heterotropic interaction with the trinucleotide comes mainly from a more favorable entropy, which indicates that distinct desolvation effects and/or changes in the conformational flexibility of Efl1 also play a determining role in the interaction affinity.

Assuming a linear dependence of ΔH_b, data in Fig. 2C yielded heat capacity changes (ΔCp_b) of −310 ± 5 and − 560 ± 23 cal mol^{-1} K^{-1} for the binding of Efl1 to MgGDP and MgGTP, respectively. Similar changes were obtained for the corresponding metal-free nucleotides (−318 ± 35 and − 700 ± 34 cal mol^{-1} K^{-1} for GDP and GTP, respectively). Consistently, analysis of the binding entropies (Fig. 2D) yielded similar ΔCp_b values to those obtained from analysis of the binding enthalpies: -385 ± 35 (GDP), −316 ± 3 (MgGDP), −750 ± 35 (GTP) and − 645 ± 4 (MgGTP) cal mol^{-1} K^{-1}.

In protein-ligand interactions, as well as in protein folding events, heat capacity changes are largely determined by the rearrangement of the solvent around the solutes, i.e., the extent of solvation/desolvation of the interacting surfaces [22–25,49,50]. A negative ΔCp_b magnitude indicates that the burial of apolar surface areas (ΔASA_{ap}) exceeds the positive contribution arising from the burial of polar surface areas (ΔASA_p). According to simple parametric models [22], ΔCp_b scales linearly with ΔASA_{ap} and ΔASA_p:

$$\Delta Cp_b = \alpha\Delta ASA_{ap} + \beta\Delta ASA_p \quad (10)$$

Furthermore, ΔCp_b can be phenomenologically dissected into two contributions, one related to the conformational changes undergone by the interacting molecules (ΔCp^{conf}) and the other associated with the amount of hidden area at the binding interface [51]. This last contribution would correspond to the observed change if the binding occurred as a rigid-body like association (ΔCp^{rb}):

Table 2
Thermodynamic cooperativity parameters for the heterotropic interaction between Mg(II) and guanine nucleotides to Efl1.

Receptor	Ligand	T (°C)	κ	Δg (kcal mol^{-1})	Δh (kcal mol^{-1})	$-T\Delta s$ (kcal mol^{-1})
Efl1		20	0.1	1.2	1.0	0.2
	GDP	25	0.2	0.9	1.0	−0.1
		30	0.4	0.6	1.1	−0.5
		20	3.8	−0.7	−0.5	−0.2
	GTP	25	1.9	−0.4	0.1	−0.5
		30	2	−0.4	0.9	−1.3

$$\Delta Cp_b = \Delta Cp^{conf} + \Delta Cp^{rb} \quad (11)$$

Estimation of ΔCp^{rb} can be achieved by analyzing the 3D structure of the complex involved and modeling the free molecules as if they adopted the same conformation as that observed in the complex. Since the cryo-EM structures of Efl1 bound to the ribosomal 60S subunit are of low resolution (> 8 Å), it was not possible to locate the nucleotide in the active site of the GTPase [14]. To estimate the area buried at a GTPase-nucleotide interface, we surveyed the PDB for high-resolution structures of nucleotide-bound translational GTPases. As detailed in the Materials and Methods section, three GTPases with GDP, four with MgGDP, two with GTP/GMPPNP and two with MgGMPPNP were found. For each nucleotide type, the average ΔASA_p and ΔASA_{ap} was calculated. The non-hydrolyzable substrate analogue GMPPNP was considered equivalent to GTP. The average ΔCp^{rb} for each nucleotide type was estimated from Eq. 10 using the aforementioned ΔASA values and the Murphy & Freire parameters $\alpha = 0.45$ and $\beta = -0.26\ cal\ mol^{-1}\ K^{-1}\ Å^{-2}$ [22]. Clearly, ΔCp^{rb} represents only a small portion of the total heat capacity binding change measured for the Efl1 complexes (Table 3, 4th column). ΔCp_b and ΔCp^{rb} were used to calculate ΔCp^{conf} (Table 3, 5th column, Eq. (11). In turn, ΔCp^{conf} relates to the total area change (ΔASA_t):

$$\Delta Cp^{conf} = 0.45 f_{ap} \Delta ASA_t - 0.26(1 - f_{ap})\Delta ASA_t \quad (12)$$

where f_{ap} represents the average hydrophobicity index ($f_{ap} = 0.68$) seen at protein-protein interfaces (Table 3, 6th column) [52–54]. Finally, assuming that each residue buries on average 47 $Å^2$ of surface area [54], the number of residues (N_{res}) sequestered from the solvent by protein conformational rearrangements was calculated (Table 3, 7th column).

The deconvolution of the ΔCp_b values revealed that upon GDP/MgGDP binding, Efl1 undergoes a conformational change accompanied by the burial of ~1200 $Å^2$ of surface area (~28 residues). GTP/MgGTP binding elicited a larger conformational change involving the burial of ~3100 $Å^2$ of surface area (~66 residues).

Since Efl1 has a very flexible structure, the possibility cannot be ruled out that a substantial fraction of the binding heat capacity arises from large changes in the conformational fluctuations of the GTPase (e.g., by "stiffening" of the protein structure) upon binding [55–57]. Therefore, the binding entropy was also analyzed as an alternative way to infer the extent of the conformational changes undergone by Efl1. ΔS_b can be dissected into three main components [58]:

$$\Delta S_b = \Delta S_{solv} + \Delta S_{conf} + \Delta S_{r-t} \quad (13)$$

The solvation entropy (ΔS_{solv}) results from changes in the degrees of freedom of the solvent molecules released from the interacting surfaces and can be calculated as follows:

$$\Delta S_{solv} = \Delta Cp_b(\ln(T/T_S)) \quad (14)$$

T_S is a reference temperature ($T = 112$ °C) where solvation effects do not contribute to the overall binding entropy [58]. $\Delta S_{r\text{-}t}$ contains the loss of overall degrees of rotation and translation, and has been estimated as $\sim -8\ cal\ mol^{-1}\ K^{-1}$ for a bimolecular association [58,59]. Accordingly, using this value and Eq. 14 (Table 3, 9th column), the conformational entropy (ΔS_{conf}) was estimated from Eq. 13 (Table 3, 10th column). In turn, the number of rotatable bonds that become frozen upon complex formation (N_{rotb}) was estimated assuming an average entropy decrease of −2 e.u. per bond [60], i.e., $N_{rotb} = -\Delta S_{conf}/2$ (Table 3, 11th column). As shown in Table 3, the N_{rotb} values for the GTP complexes are twice higher than those involved in the formation of GDP complexes, a result that is in good agreement with the deconvolution analysis of the ΔCp_b values.

3.3. Energetic effects of Sdo1 in the interaction of Efl1 with guanine nucleotides

It has been reported that Sdo1 modifies the interaction strength of Efl1 with guanine nucleotides [21]. To solve the coupled equilibria that occur in the presence of Sdo1 (Scheme 2), the protein-protein interaction was first measured by titrating Efl1 with Sdo1 (Fig. 4A). The interaction was enthalpically driven showing a favorable entropy component at 20 °C and an unfavorable one at 30 °C (Table 4). The binding parameters obtained here are in good agreement with those determined also calorimetrically by Asano et al. ($\Delta G_b = -9.9\ kcal\ mol^{-1}$, $\Delta H_b = -14.0\ kcal\ mol^{-1}$, $T\Delta S_b = -4\ kcal\ mol^{-1}$, 30 °C) [18]. Analysis of the thermal dependence of ΔH_b (ΔS_b) yielded a ΔCp_b value of -860 ± 31 (-786 ± 12) $cal\ mol^{-1}\ K^{-1}$ (Fig. 4), which, according to Eqs. 10 and 12, is consistent with the burial of ~4000 $Å^2$ (or ~80 residues). Given that the structure of the isolated Sdo1-Efl1 complex has not yet been solved, it is not possible to discern whether this overall change corresponds only to the direct protein-protein contact, or also to significant conformational changes of the molecular partners.

In another series of experiments, the pre-formed Efl1-Sdo1 complex was titrated with guanine nucleotides (Fig. 4B). These results together with those obtained for the interaction of Efl1 with nucleotides allowed the determination of the complete coupled equilibria depicted in Scheme 2. The binding of Sdo1 to Efl1 exerted disparate effects on the affinity for the nucleotides (Table 4). At 30 °C, the affinity of Sdo1-bound Efl1 for GDP decreased three times in relation to the isolated Efl1 because of an unfavorable entropy component. By contrast, Sdo1 increased the affinity of Efl1 for GTP by a factor of ~20 with a more favorable entropy change despite a larger enthalpic penalty. Therefore, Sdo1 improved the relative affinity of Efl1 for GTP over that for GDP by a factor of ~70. Because of the distinct temperature dependences on nucleotide binding, a smaller improvement (~30 times) was observed at 20 °C. Reciprocally, GDP weakened the interaction of Sdo1 and Efl1, while GTP increased the affinity between the two proteins (Fig. 5). Noteworthy, the association of GTP to the preformed Efl1-Sdo1 complex was accompanied by far smaller ΔCp_b and ΔH_b values than those observed for the isolated GTPase. Energetic-based calculations indicated that only 8 residues became buried upon docking of GTP on the protein binary complex (Table 3). Accordingly, Sdo1 seems to pre-induce a conformational change in Efl1 that makes binding to GTP an event in which the net changes in ΔASA and the number of free rotatable bonds are significantly reduced in relation to the changes observed for the isolated Efl1. Because of reciprocal effects (Fig. 5), a similar behavior is observed in the comparison of Efl1 binding to Sdo1 in the presence versus the absence of GTP ($\Delta\Delta Cp_b = 610\ cal\ mol^{-1}\ K^{-1}$).

Table 3
Energetic-based calculations of the conformational changes of Efl1 or Sdo1-Efl1 upon nucleotide binding[a].

Receptor	Ligand	ΔCp_b	ΔCp_{rb}	ΔCp^{conf}	$-\Delta ASA_t$	N_{res}	ΔS_b	ΔS_{solv}	ΔS_{conf}	N_{rotb}
Efl1	GDP	−318	−30	−288	1293	28	7	81	−67	33
	MgGDP	−310	−48	−262	1176	25	7	79	−64	32
	GTP	−700	−11	−689	3092	66	6	179	−165	82
	MgGTP	−560	−25	−535	2401	51	7	143	−128	64
Efl1-Sdo1	GDP	−640	−30	−610	2738	58	7	164	−149	74
	GTP	−90	−11	−79	355	8	18	23	3	1

[a] Units for ΔCp and ΔS correspond to $cal\ mol^{-1}\ K^{-1}$ and for ΔASA to $Å^2$.

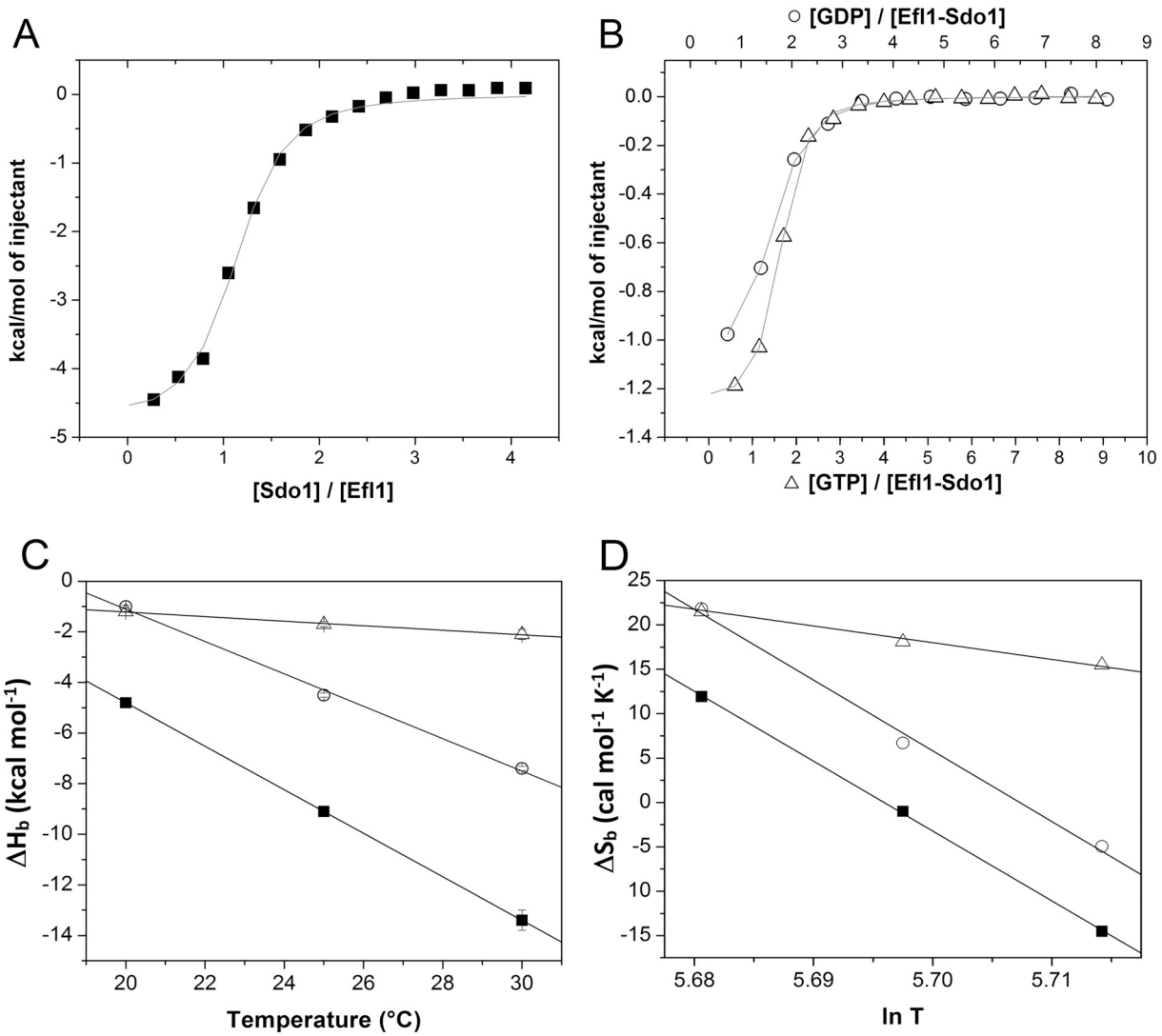

Fig. 4. Calorimetric characterization of the binding of Efl1 to Sdo1 (■), and the complex Sdo1-Efl1 to GDP (○) or GTP (△). (A-B) Binding isotherms at 20 °C. (C-D) Binding enthalpy and entropy as a function of temperature. Dashed lines correspond to the least-squares linear fittings describing the thermal dependence of ΔH_b or ΔS_b.

Table 4
Thermodynamic parameters for the ternary binding system formed between Efl1, Sdo1 and guanine nucleotides determined by ITC.

Receptor	Ligand	T (°C)	n	K_b (mM^{-1})	K_d (μM)	ΔG_b (kcal mol^{-1})	ΔH_b (kcal mol^{-1})	$-T\Delta S_b$ (kcal mol^{-1})	ΔCp_b (cal mol^{-1} K^{-1})
Efl1	Sdo1	20	1.07 ± 0.02	1580 ± 280	0.6 ± 0.0	−8.3	−4.8 ± 0.1	−3.5	
		25	0.87 ± 0.02	3200 ± 650	0.3 ± 0.0	−8.8	−9.1 ± 0.2	0.3	−860 ± 31
		30	0.87 ± 0.05	3110 ± 630	0.3 ± 0.0	−9.0	−13.4 ± 0.4	4.4	
Sdo1-Efl1	GDP	20	1.30 ± 0.02	330 ± 38	3 ± 1	−7.4	−1.0 ± 0.1	−6.4	
		25	0.93 ± 0.03	62 ± 3	16 ±	−6.5	−4.5 ± 0.0	−2.0	−640 ± 34
		30	1.01 ± 0.00	19 ± 1	52 ± 1	−5.9	−7.4 ± 0.0	1.5	
	GTP	20	1.03 ± 0.00	481 ± 27	2 ± 0	−7.6	−1.2 ± 0.0	−6.4	
		25	1.10 ± 0.02	166 ± 13	6 ± 1	−7.1	−1.7 ± 0.1	−5.4	−90 ± 5
		30	1.03 ± 0.00	89 ± 12	11 ± 1	−6.8	−2.1 ± 0.2	−4.7	

This picture is consistent with the cooperativity parameter values, which indicate that the effect of Sdo1 at favoring the interaction of Efl1 with GTP is of entropic origin (Table 5). On the contrary, the associated ΔCp_b value of GDP binding to Efl1 was twice larger in the presence than in the absence of Sdo1 (Table 4). Similarly, Sdo1 binding to the Efl1-GDP complex was accompanied by a larger heat capacity decrease ($\Delta\Delta Cp_b = -322$ cal mol^{-1} K^{-1}), which indicates the additional burial of 31 residues in relation to the binding to the isolated enzyme.

4. Discussion

Nucleotide-dependent conformational changes play a central role in the regulation and function of GTPases [61–63]. As a general rule, these enzymes adopt a more compact conformation in complex with GTP (the so-called T form) than that with GDP (the so-called D form) [64–67]. According to the extent of the structural rearrangements inferred from the analysis of the binding heat capacities and entropies, Efl1 parallels

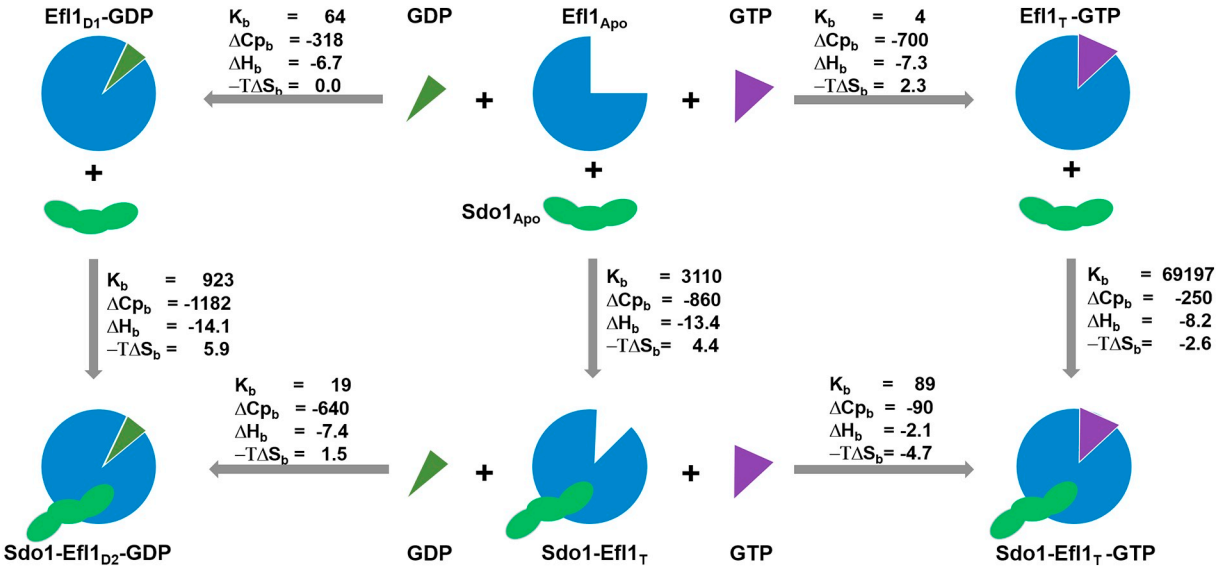

Fig. 5. Energetics of the coupled equilibria between Efl1, Sdo1 and guanine nucleotides. The analysis of the binding parameters indicates that Efl1 exhibits a significant structural plasticity adopting at least four different conformational states: the apo form of the enzyme ($Efl1_{Apo}$), a T-like conformation interacting with GTP and/or Sdo1 ($Efl1_{T}$), a D-like conformation bound to GDP alone ($Efl1_{D1}$) that undergoes a large conformational change upon binding to Sdo1 ($Efl1_{D2}$). Units: K_b in mM^{-1}, ΔH_b and $-T\Delta S_b$ in kcal mol^{-1}, ΔCp_b in cal mol^{-1} K^{-1}.

Table 5
Thermodynamic cooperativity parameters for the heterotropic interaction of Efl1 to Sdo1 and guanine nucleotides.

Receptor	Ligand	Temperature °C	κ	Δg kcal mol^{-1}	Δh kcal mol^{-1}	-TΔs kcal mol^{-1}
Efl1-Sdo1	GDP	20	1.2	−0.1	2.5	−2.6
		25	0.4	0.5	0.5	0.0
		30	0.3	0.8	−0.7	1.5
	GTP	20	40.1	−2.1	2.1	−1.2
		25	20.8	−1.8	1.8	−3.6
		30	22.3	−1.8	5.2	−7.0

this behavior by burying 51–66 residues when bound to GTP versus 25–28 when interacting with GDP. It is plausible that in analogy to other GTPases, the conformational changes that lead to the burial of those residues are mainly associated with the restructuring of switches 1 and 2 in the G domain [61]. The heterotropic cooperative parameters indicate that Mg(II) modifies slightly GT(D)P binding to Efl1, showing the same trends observed in translational GTPases. Binding of GTP to the pre-formed Sdo1-Efl1 complex involves the burial of a small number of residues suggesting a rigid-body like association. Therefore, it seems that Sdo1 brings Efl1 to adopt a T-like conformation, with the concomitant affinity gain for the guanine trinucleotide. In contrast, the binding of GDP to the Sdo1-Efl1 complex is accompanied by a large decrease in heat capacity, indicating that Efl1 and/or Sdo1 in the GDP complex adopt a significantly different and less stable conformational state in relation to the Sdo1-Efl1-GTP complex. Overall, the present analysis suggests that Efl1 off the ribosome can adopt at least four clearly differentiable conformational states, namely, 1) the apo form, 2) a T-like conformation that can be achieved by the interaction with GTP ($Efl1_{T}$-GTP), with Sdo1 (Sdo1-$Efl1_{T}$) or with both molecules (Sdo1-$Efl1_{T}$-GTP), 3) a D-like conformation in presence of GDP alone ($Efl1_{D1}$-GDP), and 4) a different D-like conformation induced by the simultaneous effect of Sdo1 and GDP (Sdo1-$Efl1_{D2}$-GDP) (Fig. 5). Therefore, Efl1 exhibits a larger conformational plasticity compared to the classical GTPases whose GTP- and GDP-bound structures are distinct and correspond to their active and inactive forms.

To what extent the large conformational plasticity exhibited by Efl1 in solution and the binding modes of this GTPase with Sdo1 and nucleotides is transferable to the ribosomal context is a question still to be answered. The available cryo-EM models establish a binding mode on the ribosome in which domains II-III of SBDS interact directly with domains III-IV of EFL1, while the insertion loop within domain II of the GTPase is far away from the cofactor [14]. This binding posture locates the SDS-related residue Sdo1 Ser^{143} far away from the Sdo1-Efl1 interface. In contrast, the binding mode derived from interaction data in a ribosome-free context establishes that Efl1 interacts with Sdo1 in an inverted orientation with respect to the complex on the ribosome, making direct contact with the cofactor through the insertion loop [18,20] with Ser^{143} positioned within the Sdo1-Efl1 interface. The calorimetric results presented herein clearly indicate that the interaction of Efl1 with GT(D)P and Mg(II) remarkably resembles that observed for other GTPases, and that Sdo1 behaves as an accessory factor that induces classical energetic and structural effects that favor the interaction of the GTPase with the trinucleotide and weaken the interaction with the dinucleotide. In view of these characteristic effects, it is difficult to conclude that the interaction of Sdo1 and Efl1 off the ribosome is fortuitous.

The proposed main role of SBDS/Sdo1 is to facilitate a conformational transition in EFL1/Efl1 that sterically displaces eIF6/Tif6 from the ribosomal subunit [14]. However, on the basis of the biochemical data available, other conceivable functions for this cofactor could be invoked. For instance, titration experiments have shown that EFL1 can bind mature 60S subunits independently of SBDS, suggesting that the cofactor does not play a significant role as a recruiter of the GTPase to the ribosomal subunit [5]. There is no experimental evidence describing the binding events to the isolated 60S subunit and it is not clear whether EFL1 and SBDS bind as heterodimer or the binding hierarchy of the isolated proteins. If EFL1 emulates the behavior of EF-G/EF-2 and other translation GTPases [68], it would be expected to adopt a T-like

conformation to interact with the ribosomal subunit. Accordingly, our calorimetric analysis clearly shows that the Efl1 T-like conformation is largely stabilized by Sdo1. Furthermore, since Efl1 and its cofactor are cytoplasmic proteins that interact to each other in presence of GTP with low nanomolar affinity (Fig. 5), they may bind to the 60S subunit as a heterodimer. It has been proposed that eviction of eIF6 precedes the release of SBDS and EFL1 that is necessary to produce fully mature 60S subunits [14]. Presumably, this release is associated with a conformational change driven by GTP hydrolysis, which decreases the affinity of the SBDS-EFL1 binomial for the ribosomal subunit. Consistent with this scenario, our data revealed that the conformations of the Sdo1-Efl1$_{D2}$-GDP and Sdo1-Efl1$_{T}$-GTP complexes differ significantly from each other. Therefore, the large conformational transition from Sdo1-Efl1$_{T}$-GTP to Sdo1-Efl1$_{D2}$-GDP triggered by GTP hydrolysis could facilitate the subsequent release of the assembly factors.

In a previous study, it was proposed that Sdo1 acts as a GDP exchange factor or GEF for Efl1 [21,69]. Consistently, the results obtained herein indicate that Sdo1 significantly increases Efl1's affinity for GTP over GDP; an effect elicited by simultaneously decreasing the affinity for GDP and increasing that for GTP. However, when compared to the behavior observed for other GTPases that are strongly dependent on the GEF partner to displace GDP [70–72], it seems that the role of Sdo1 as an exchange factor is marginal in kinetic terms. In fact, Efl1 exchanges nucleotides at a rate comparable to that of GTPases that do not require a GEF partner [73,74]. Nevertheless, it is worth noting that the dissociation constants of Efl1-nucleotide complexes are within the low-to-medium micromolar ranges, which in turn are close to the concentrations of GDP and GTP observed in vivo. In exponential growing cells, the *S. cerevisiae* intracellular concentrations of GTP and GDP are ~200 and ~50 μM, respectively [75]. Under this condition, the interaction of Sdo1 with Efl1 would favor the GTP-bound form of the enzyme by a factor of 18 over the apo or GDP-bound forms. Conversely, the apo, GTP-bound and GDP-bound Efl1 forms would coexist in the cytoplasm almost equimolarly in the absence of Sdo1. If this GTPase, as exhibited by other related GTPases, needs to be preloaded with GTP to interact with the 60S subunit, Sdo1 could modulate the relative populations of the Efl1 forms and, as a consequence, affect the final incorporation rate of the 60S subunits into the pool of active ribosomes.

In conclusion, the structural and energetic effects elicited by Sdo1 and guanine nucleotides modulate in a very specific and robust way the complex conformational landscape of Efl1 in solution, certainly recalling the behavior of other GTPases. Clearly, the drastically different binding modes inferred for the interaction of Sdo1/SBDS and Efl1/EFL1 on and off the ribosome pose a significant conundrum. In particular, this is because the GTP-bound conformation of Efl1 (required for the binding of the GTPase on the 60S subunit surface) is largely stabilized by isolated Sdo1. Further research is clearly warranted in order to reconcile the GTPase-cofactor binding modes determined from the solution and cryo-EM data.

Acknowledgements

Axel Luviano is a doctoral student from Programa de Doctorado en Ciencias Biomédicas, Universidad Nacional Autónoma de México (UNAM) and received fellowship No. 269390 from CONACyT. We thank Dr. Patricia Cano-Sánchez, Q. Rocío Patiño Maya and Dr. Guillermo Salcedo for the technical support in the production of the recombinant proteins, CD and calorimetric measurements, respectively. This work was financed in part by DGAPA, UNAM [PAPIIT IN205018] and CONACyT [Grants 235831, 283909].

References

[1] J. de la Cruz, K. Karbstein, J.L. Woolford, Functions of ribosomal proteins in assembly of eukaryotic ribosomes in vivo, Annu. Rev. Biochem. 84 (2015) 93–129, https://doi.org/10.1146/annurev-biochem-060614-033917.

[2] S. Gerhardy, A.M. Menet, C. Peña, J.J. Petkowski, V.G. Panse, Assembly and nuclear export of pre-ribosomal particles in budding yeast, Chromosoma 123 (2014) 327–344, https://doi.org/10.1007/s00412-014-0463-z.

[3] P. Nerurkar, M. Altvater, S. Gerhardy, S. Schütz, U. Fischer, C. Weirich, V.G. Panse, Eukaryotic ribosome assembly and nuclear export, Int. Rev. Cell Mol. Biol. (2015) 107–140 (doi:10.1016/bs.ircmb.2015.07.002).

[4] M. Ceci, C. Gaviraghi, C. Gorrini, L.A. Sala, N. Offenhäuser, P. Carlo Marchisio, S. Biffo, Release of eIF6 (p27BBP) from the 60S subunit allows 80S ribosome assembly, Nature 426 (2003) 579–584, https://doi.org/10.1038/nature02160.

[5] A.J. Finch, C. Hilcenko, N. Basse, L.F. Drynan, B. Goyenechea, T.F. Menne, A. González Fernández, P. Simpson, C.S. D'Santos, M.J. Arends, J. Donadieu, C. Bellanné-Chantelot, M. Costanzo, C. Boone, A.N. McKenzie, S.M.V. Freund, A.J. Warren, Uncoupling of GTP hydrolysis from eIF6 release on the ribosome causes Shwachman-Diamond syndrome, Genes Dev. 25 (2011) 917–929 (doi:10.1101/gad.623011).

[6] T.F. Menne, B. Goyenechea, N. Sánchez-Puig, C.C. Wong, L.M. Tonkin, P.J. Ancliff, R.L. Brost, M. Costanzo, C. Boone, A.J. Warren, The Shwachman-Bodian-Diamond syndrome protein mediates translational activation of ribosomes in yeast, Nat. Genet. 39 (2007) 486–495, https://doi.org/10.1038/ng1994.

[7] A.J. Warren, Molecular basis of the human ribosomopathy Shwachman-Diamond syndrome, Adv. Biol. Regul. 67 (2018) 109–127, https://doi.org/10.1016/j.jbior.2017.09.002.

[8] G.R.B. Boocock, J.A. Morrison, M. Popovic, N. Richards, L. Ellis, P.R. Durie, J.M. Rommens, Mutations in SBDS are associated with Shwachman–Diamond syndrome, Nat. Genet. 33 (2003) 97–101, https://doi.org/10.1038/ng1062.

[9] P. Stepensky, M. Chacón-Flores, K.H. Kim, O. Abuzaitoun, A. Bautista-Santos, N. Simanovsky, D. Siliqi, D. Altamura, A. Méndez-Godoy, A. Gijsbers, A. Naser Eddin, T. Dor, J. Charrow, N. Sánchez-Puig, O. Elpeleg, Mutations in *EFL1*, an *SBDS* partner, are associated with infantile pancytopenia, exocrine pancreatic insufficiency and skeletal anomalies in aShwachman-Diamond like syndrome, J. Med. Genet. 54 (2017) 558–566, https://doi.org/10.1136/jmedgenet-2016-104366.

[10] Q.K.-G. Tan, H. Cope, R.C. Spillmann, N. Stong, Y.-H. Jiang, M.T. McDonald, J.A. Rothman, M.W. Butler, D.P. Frush, R.S. Lachman, B. Lee, C.A. Bacino, M.J. Bonner, C.M. McCall, A.A. Pendse, N. Walley, U. members, V. Shashi, L.D.M. Pena, Further evidence for the involvement of *EFL1* in a Shwachman-Diamond-like syndrome and expansion of the phenotypic features, Mol. Case Stud. (2018), https://doi.org/10.1101/mcs.a003046 mcs.a003046.

[11] B. Senger, D.L. Lafontaine, J.S. Graindorge, O. Gadal, A. Camasses, A. Sanni, J.M. Garnier, M. Breitenbach, E. Hurt, F. Fasiolo, The nucle(ol)ar Tif6p and Efl1p are required for a late cytoplasmic step of ribosome synthesis, Mol. Cell 8 (2001) 1363–1373 http://www.ncbi.nlm.nih.gov/pubmed/11779510 (accessed December 10, 2018), https://doi.org/10.1016/S1097-2765(01)00403-8.

[12] A. Savchenko, N. Krogan, J.R. Cort, E. Evdokimova, J.M. Lew, A.A. Yee, L. Sánchez-Pulido, M.A. Andrade, A. Bochkarev, J.D. Watson, M.A. Kennedy, J. Greenblatt, T. Hughes, C.H. Arrowsmith, J.M. Rommens, A.M. Edwards, The Shwachman-Bodian-Diamond syndrome protein family is involved in RNA metabolism, J. Biol. Chem. 280 (2005) 19213–19220, https://doi.org/10.1074/jbc.M414421200.

[13] C. Shammas, T.F. Menne, C. Hilcenko, S.R. Michell, B. Goyenechea, G.R.B. Boocock, P.R. Durie, J.M. Rommens, A.J. Warren, Structural and mutational analysis of the SBDS protein family. Insight into the leukemia-associated Shwachman-Diamond syndrome, J. Biol. Chem. 280 (2005) 19221–19229, https://doi.org/10.1074/jbc.M414656200.

[14] F. Weis, E. Giudice, M. Churcher, L. Jin, C. Hilcenko, C.C. Wong, D. Traynor, R.R. Kay, A.J. Warren, Mechanism of eIF6 release from the nascent 60S ribosomal subunit, Nat. Struct. Mol. Biol. 22 (2015) 914–919, https://doi.org/10.1038/nsmb.3112.

[15] K.-Y. Lo, Z. Li, C. Bussiere, S. Bresson, E.M. Marcotte, A.W. Johnson, Defining the pathway of cytoplasmic maturation of the 60S ribosomal subunit, Mol. Cell 39 (2010) 196–208, https://doi.org/10.1016/j.molcel.2010.06.018.

[16] A.G. Malyutin, S. Musalgaonkar, S. Patchett, J. Frank, A.W. Johnson, Nmd3 is a structural mimic of eIF5A, and activates the cpGTPase Lsg1 during 60S ribosome biogenesis, EMBO J. 36 (2017) 854–868, https://doi.org/10.15252/embj.201696012.

[17] S. Patchett, S. Musalgaonkar, A.G. Malyutin, A.W. Johnson, The T-cell leukemia related rpl10-R98S mutant traps the 60S export adapter Nmd3 in the ribosomal P site in yeast, PLoS Genet. 13 (2017) e1006894, , https://doi.org/10.1371/journal.pgen.1006894.

[18] N. Asano, H. Atsuumi, A. Nakamura, Y. Tanaka, I. Tanaka, M. Yao, Direct interaction between EFL1 and SBDS is mediated by an intrinsically disordered insertion domain, Biochem. Biophys. Res. Commun. 443 (2014) 1251–1256, https://doi.org/10.1016/j.bbrc.2013.12.143.

[19] A. Gijsbers, D. Montagut, A. Méndez-Godoy, D. Altamura, M. Saviano, D. Siliqi, N. Sánchez-Puig, Interaction of the GTPase elongation factor Like-1 with the Shwachman-Diamond syndrome protein and its missense mutations, Int. J. Mol. Sci. 19 (2018) 4012, https://doi.org/10.3390/ijms19124012.

[20] A.N. Holding, XL-MS: protein cross-linking coupled with mass spectrometry, Methods 89 (2015) 54–63, https://doi.org/10.1016/j.ymeth.2015.06.010.

[21] A. García-Márquez, A. Gijsbers, E. de la Mora, N. Sánchez-Puig, Defective guanine nucleotide exchange in the elongation factor-like 1 (EFL1) GTPase by mutations in the Shwachman-Diamond syndrome protein, J. Biol. Chem. 290 (2015) 17669–17678, https://doi.org/10.1074/jbc.M114.626275.

[22] K.P. Murphy, E. Freire, Thermodynamics of structural stability and cooperative folding behavior in proteins, Adv. Protein Chem. 43 (1992) 313–361.

[23] G. Pérez-Hernández, E. García-Hernández, R.A.R.A. Zubillaga, M.T.M.T. De Gómez-Puyou, Structural energetics of MgADP binding to the isolated β subunit of F1-ATPase from thermophilic Bacillus PS3, Arch. Biochem. Biophys. 408 (2002)

177–183, https://doi.org/10.1016/S0003-9861(02)00577-5.
[24] N.V. Prabhu, K.A. Sharp, Heat capacity in proteins, Annu. Rev. Phys. Chem. 56 (2005) 521–548, https://doi.org/10.1146/annurev.physchem.56.092503.141202.
[25] S. Vega, O. Abian, A. Velazquez-Campoy, On the link between conformational changes, ligand binding and heat capacity, Biochim. Biophys. Acta 1860 (2016) 868–878, https://doi.org/10.1016/j.bbagen.2015.10.010.
[26] A. Gijsbers, T. Nishigaki, N. Sánchez-Puig, Fluorescence anisotropy as a tool to study protein-protein interactions, J. Vis. Exp. (2016), https://doi.org/10.3791/54640.
[27] T.W. Christianson, R.S. Sikorski, M. Dante, J.H. Shero, P. Hieter, Multifunctional yeast high-copy-number shuttle vectors, Gene 110 (1992) 119–122 http://www.ncbi.nlm.nih.gov/pubmed/1544568 (accessed December 10, 2018), https://doi.org/10.1016/0378-1119(92)90454-W.
[28] C. Louis-Jeune, M.A. Andrade-Navarro, C. Perez-Iratxeta, Prediction of protein secondary structure from circular dichroism using theoretically derived spectra, Proteins 80 (2012) 374–381, https://doi.org/10.1002/prot.23188.
[29] N.O. Pulido, G. Salcedo, G. Pérez-Hernández, C. José-Núñez, A. Velázquez-Campoy, E. García-Hernández, Energetic effects of magnesium in the recognition of adenosine nucleotides by the F 1 -ATPase β subunit, Biochemistry 49 (2010) 5258–5268, https://doi.org/10.1021/bi1006767.
[30] N.O. Pulido, E.A. Chavelas, F. Turner, E. García-Hernández, Current applications of isothermal titration calorimetry to the study of protein complexes, in: E. García-Hernández, D.A. Fernández-Velasco (Eds.), Adv. Protein Phys. Chem., Transworld Research Network, India, 2008, pp. 115–138.
[31] A. Velazquez-Campoy, S.A. Leavitt, E. Freire, Characterization of protein–protein interactions by isothermal titration calorimetry, Protein-Protein Interact., Humana Press, New Jersey, 2004, pp. 035–054 (doi:10.1385/1-59259-762-9:035).
[32] E. Muñoz, A. Piñeiro, AFFINImeter software: from its beginnings to future trends- a literature review, J. Appl. Bioanal. 4 (2018) 124–139, https://doi.org/10.17145/jab.18.017.
[33] S. al-Karadaghi, A. Aevarsson, M. Garber, J. Zheltonosova, A. Liljas, The structure of elongation factor G in complex with GDP: conformational flexibility and nucleotide exchange, Structure 4 (1996) 555–565 http://www.ncbi.nlm.nih.gov/pubmed/8736554 (accessed February 8, 2018), https://doi.org/10.1016/S0969-2126(96)00061-5.
[34] M. Dobosz-Bartoszek, M.H. Pinkerton, Z. Otwinowski, S. Chakravarthy, D. Söll, P.R. Copeland, M. Simonovic, Crystal structures of the human elongation factor eEFSec suggest a non-canonical mechanism for selenocysteine incorporation, Nat. Commun. 7 (2016) 12941, , https://doi.org/10.1038/ncomms12941.
[35] A.M.G. van den Elzen, J. Henri, N. Lazar, M.E. Gas, D. Durand, F. Lacroute, M. Nicaise, H. van Tilbeurgh, B. Séraphin, M. Graille, Dissection of Dom34–Hbs1 reveals independent functions in two RNA quality control pathways, Nat. Struct. Mol. Biol. 17 (2010) 1446–1452, https://doi.org/10.1038/nsmb.1963.
[36] M. Laurberg, O. Kristensen, K. Martemyanov, A.T. Gudkov, I. Nagaev, D. Hughes, A. Liljas, Structure of a mutant EF-G reveals domain III and possibly the fusidic acid binding site 1 1Edited by I. A. Wilson, J. Mol. Biol. 303 (2000) 593–603, https://doi.org/10.1006/jmbi.2000.4168.
[37] G. Polekhina, S. Thirup, M. Kjeldgaard, P. Nissen, C. Lippmann, J. Nyborg, Helix unwinding in the effector region of elongation factor EF-Tu-GDP., Structure 4 (1996) 1141–51. http://www.ncbi.nlm.nih.gov/pubmed/8939739 (accessed May 12, 2018), doi: https://doi.org/10.1016/S0969-2126(96)00122-0.
[38] B. Kuhle, R. Ficner, EIF5B employs a novel domain release mechanism to catalyze ribosomal subunit joining, EMBO J. 33 (2014) 1177–1191, https://doi.org/10.1002/embj.201387344.
[39] R. Søe, R.T. Mosley, M. Justice, J. Nielsen-Kahn, M. Shastry, A.R. Merrill, G.R. Andersen, Sordarin derivatives induce a novel conformation of the yeast ribosome translocation factor eEF2, J. Biol. Chem. 282 (2007) 657–666, https://doi.org/10.1074/jbc.M607830200.
[40] M. Kjeldgaard, P. Nissen, S. Thirup, J. Nyborg, The crystal structure of elongation factor EF-Tu from Thermus aquaticus in the GTP conformation., Structure 1 (1993) 35–50. http://www.ncbi.nlm.nih.gov/pubmed/8069622 (accessed May 12, 2018), doi: https://doi.org/10.1016/0969-2126(93)90007-4.
[41] J. Mesters, R. Hilgenfeld, T. Hogg, Insights into the GTPase mechanism of EF-Tu from structural studies, The Ribosome, American Society of Microbiology, 2000, pp. 347–357, , https://doi.org/10.1128/9781555818142.ch28.
[42] T. Yanagisawa, R. Ishii, Y. Hikida, R. Fukunaga, T. Sengoku, S. Sekine, S. Yokoyama, A SelB/EF-Tu/aIF2γ-like protein from Methanosarcina mazei in the GTP-bound form binds cysteinyl-tRNACys, J. Struct. Funct. Genom. 16 (2015) 25–41, https://doi.org/10.1007/s10969-015-9193-6.
[43] S.J. Hubbard, J.M. Thornton, "NACCESS", Computer Program, Department of Biochemistry and Molecular Biology, 1993.
[44] O. Hahn-Herrera, G. Salcedo, X. Barril, E. García-Hernández, Inherent conformational flexibility of F1-ATPase α-subunit, Biochim. Biophys. Acta Bioenerg. 1857 (2016), https://doi.org/10.1016/j.bbabio.2016.04.283.
[45] G. Salcedo, P. Cano-Sánchez, M.T.M.T. De Gómez-Puyou, A. Velázquez-Campoy, E. García-Hernández, Isolated noncatalytic and catalytic subunits of F1-ATPase exhibit similar, albeit not identical, energetic strategies for recognizing adenosine nucleotides, Biochim. Biophys. Acta Bioenerg. 1837 (2014) 44–50, https://doi.org/10.1016/j.bbabio.2013.08.005.
[46] A. Velazquez-Campoy, Allostery and cooperative interactions in proteins assessed by isothermal titration calorimetry, in: M. Bastos (Ed.), Biocalorimetry - Found. Contemp. Approaches, CRC Press, Boca Raton, 2016, pp. 223–246.
[47] R.N. Goldberg, N. Kishore, R.M. Lennen, Thermodynamic Quantities for the Ionization Reactions of Buffers, https://www.nist.gov/sites/default/files/documents/srd/jpcrd615.pdf, (2002) (accessed January 22, 2019).
[48] V.A. Mitkevich, A.V. Kononenko, I.Y. Petrushanko, D.V. Yanvarev, A.A. Makarov, L.L. Kisselev, Termination of translation in eukaryotes is mediated by the quaternary eRF1*eRF3*GTP*Mg2+ complex. The biological roles of eRF3 and prokaryotic RF3 are profoundly distinct, Nucleic Acids Res. 34 (2006) 3947–3954, https://doi.org/10.1093/nar/gkl549.
[49] E.A.E.A. Chavelas, E. García-Hernández, Heat capacity changes in carbohydrates and protein-carbohydrate complexes, Biochem. J. 420 (2009) 239–247, https://doi.org/10.1042/BJ20082171.
[50] P.L. Privalov, G.I. Makhatadze, Contribution of hydration and non-covalent interactions to the heat capacity effect on protein unfolding, J. Mol. Biol. 224 (1992) 715–723 http://www.ncbi.nlm.nih.gov/pubmed/1314903 (accessed April 14, 2017), https://doi.org/10.1016/0022-2836(92)90555-X.
[51] J.E. Ladbury, M.A. Williams, The extended interface: measuring non-local effects in biomolecular interactions, Curr. Opin. Struct. Biol. 14 (2004) 562–569, https://doi.org/10.1016/j.sbi.2004.08.001.
[52] E. García-Hernández, R.A. Zubillaga, A. Rodríguez-Romero, A. Hernández-Arana, Stereochemical metrics of lectin-carbohydrate interactions: comparison with protein-protein interfaces, Glycobiology 10 (2000) 993–1000, https://doi.org/10.1093/glycob/10.10.993.
[53] S. Jones, J.M. Thornton, Principles of protein-protein interactions, Proc. Natl. Acad. Sci. U. S. A. 93 (1996) 13–20 http://www.ncbi.nlm.nih.gov/pubmed/8552589 (accessed April 14, 2017).
[54] W.E. Stites, Protein−Protein Interactions: Interface Structure, Binding Thermodynamics, and Mutational Analysis, (1997), https://doi.org/10.1021/CR960387H.
[55] M.J. Seewald, K. Pichumani, C. Stowell, B.V. Tibbals, L. Regan, M.J. Stone, The role of backbone conformational heat capacity in protein stability: temperature dependent dynamics of the B1 domain of *Streptococcal* protein G, Protein Sci. 9 (2000) 1177–1193, https://doi.org/10.1110/ps.9.6.1177.
[56] D. Idiyatullin, I. Nesmelova, V.A. Daragan, K.H. Mayo, Heat capacities and a snapshot of the energy landscape in protein GB1 from the pre-denaturation temperature dependence of backbone NH nanosecond fluctuations, J. Mol. Biol. 325 (2003) 149–162 http://www.ncbi.nlm.nih.gov/pubmed/12473458 (accessed January 23, 2019), https://doi.org/10.1016/S0022-2836(02)01155-5.
[57] V.L. Arcus, C.R. Pudney, Change in heat capacity accurately predicts vibrational coupling in enzyme catalyzed reactions, FEBS Lett. 589 (2015) 2200–2206, https://doi.org/10.1016/j.febslet.2015.06.042.
[58] S.P. Edgcomb, K.P. Murphy, Structural energetics of protein folding and binding, Curr. Opin. Biotechnol. 11 (2000) 62–66, https://doi.org/10.1016/S0958-1669(99)00055-5.
[59] E. García-Hernández, A. Hernández-Arana, Structural bases of lectin-carbohydrate affinities: comparison with protein-folding energetics, Protein Sci. 8 (1999) 1075–1086, https://doi.org/10.1110/ps.8.5.1075.
[60] A. Doig, M. Sternberg, Side-chain conformational entropy in protein folding, Protein Sci. 4 (1995) 2247–2251, https://doi.org/10.1002/pro.5560041101.
[61] J. Cherfils, M. Zeghouf, Chronicles of the GTPase switch, Nat. Chem. Biol. 7 (2011) 493–495, https://doi.org/10.1038/nchembio.608.
[62] I.R. Vetter, A. Wittinghofer, The guanine nucleotide-binding switch in three dimensions, Science 80 (294) (2001) 1299–1304, https://doi.org/10.1126/science.1062023.
[63] A. Wittinghofer, I.R. Vetter, Structure-function relationships of the G domain, a canonical switch motif, Annu. Rev. Biochem. 80 (2011) 943–971, https://doi.org/10.1146/annurev-biochem-062708-134043.
[64] V. Hauryliuk, S. Hansson, M. Ehrenberg, Cofactor dependent conformational switching of GTPases, Biophys. J. 95 (2008) 1704–1715, https://doi.org/10.1529/biophysj.107.127290.
[65] V. Hauryliuk, V.A. Mitkevich, A. Draycheva, S. Tankov, V. Shyp, A. Ermakov, A.A. Kulikova, A.A. Makarov, M. Ehrenberg, Thermodynamics of GTP and GDP binding to bacterial initiation factor 2 suggests two types of structural transitions, J. Mol. Biol. 394 (2009) 621–626, https://doi.org/10.1016/j.jmb.2009.10.015.
[66] V. Hauryliuk, V. a Mitkevich, N. a Eliseeva, I.Y. Petrushanko, M. Ehrenberg, A. a Makarov, The pretranslocation ribosome is targeted by GTP-bound EF-G in partially activated form, Proc. Natl. Acad. Sci. U. S. A. 105 (2008) 15678–15683, https://doi.org/10.1073/pnas.0807912105.
[67] A. Paleskava, A.L. Konevega, M.V. Rodnina, Thermodynamics of the GTP-GDP-operated conformational switch of selenocysteine-specific translation factor SelB, J. Biol. Chem. 287 (2012) 27906–27912, https://doi.org/10.1074/jbc.M112.366120.
[68] V.A. Mitkevich, V. Shyp, I.Y. Petrushanko, A. Soosaar, G.C. Atkinson, T. Tenson, A.A. Makarov, V. Hauryliuk, GTPases IF2 and EF-G bind GDP and the SRL RNA in a mutually exclusive manner, Sci. Rep. 2 (2012) 843, , https://doi.org/10.1038/srep00843.
[69] A. Gijsbers, A. García-Márquez, A. Luviano, N. Sánchez-Puig, Guanine nucleotide exchange in the ribosomal GTPase EFL1 is modulated by the protein mutated in the Shwachman–Diamond syndrome, Biochem. Biophys. Res. Commun. 437 (2013) 349–354, https://doi.org/10.1016/j.bbrc.2013.06.077.
[70] R. Goody, W. Hofmann-Goody, Exchange factors, effectors, GAPs and motor proteins: common thermodynamic and kinetic principles for different functions, Eur. Biophys. J. 31 (2002) 268–274, https://doi.org/10.1007/s00249-002-0225-3.
[71] K.B. Gromadski, T. Schümmer, A. Strømgaard, C.R. Knudsen, T.G. Kinzy, M.V. Rodnina, Kinetics of the interactions between yeast elongation factors 1A and 1Balpha, guanine nucleotides, and aminoacyl-tRNA, J. Biol. Chem. 282 (2007)

35629–35637, https://doi.org/10.1074/jbc.M707245200.
[72] K.B. Gromadski, H.-J. Wieden, M.V. Rodnina, Kinetic mechanism of elongation factor Ts-catalyzed nucleotide exchange in elongation factor Tu, Biochemistry 41 (2002) 162–169 http://www.ncbi.nlm.nih.gov/pubmed/11772013 (accessed March 15, 2018), https://doi.org/10.1021/bi015712w.
[73] M. Thanbichler, A. Böck, R.S. Goody, Kinetics of the interaction of translation factor SelB from *Escherichia coli* with guanosine nucleotides and Selenocysteine insertion sequence RNA, J. Biol. Chem. 275 (2000) 20458–20466, https://doi.org/10.1074/jbc.M002496200.
[74] B. Wilden, A. Savelsbergh, M.V. Rodnina, W. Wintermeyer, Role and timing of GTP binding and hydrolysis during EF-G-dependent tRNA translocation on the ribosome, Proc. Natl. Acad. Sci. 103 (2006) 13670–13675, https://doi.org/10.1073/pnas.0606099103.
[75] S. Rudoni, S. Colombo, P. Coccetti, E. Martegani, Role of guanine nucleotides in the regulation of the Ras/cAMP pathway in Saccharomyces cerevisiae, Biochim. Biophys. Acta 1538 (2001) 181–189 http://www.ncbi.nlm.nih.gov/pubmed/11336789 (accessed October 3, 2017).